

PROCEEDINGS OF SPIE

SPIDigitalLibrary.org/conference-proceedings-of-spie

Irritation-free optical 3D-based measurement of tidal volume

Christoph Munkelt, Matthias Heinze, Simon Schindwolf, Stefan Heist, Gunther Notni

Christoph Munkelt, Matthias Heinze, Simon Schindwolf, Stefan Heist, Gunther Notni, "Irritation-free optical 3D-based measurement of tidal volume," Proc. SPIE 11787, Automated Visual Inspection and Machine Vision IV, 117870A (20 June 2021); doi: 10.1117/12.2592714

SPIE.

Event: SPIE Optical Metrology, 2021, Online Only

Irritation-free optical 3D-based measurement of tidal volume

Christoph Munkelt^{*a}, Matthias Heinze^a, Simon Schindewolf^a, Stefan Heist^a, Gunther Notni^{ab}

^aImaging and Sensor Department, Fraunhofer Institute for Applied Optics and Precision Engineering IOF, Albert-Einstein-Str. 7, 07745 Jena, Germany; ^bQuality Assurance and Industrial Image Processing Group, Technical University Ilmenau, Gustav-Kirchhoff-Platz 2, 98693 Ilmenau, Germany

ABSTRACT

The measurement of breathing biomechanics, such as tidal volume, can be used to assess both the breathing performance and the respiratory health of individuals. State-of-the-art methods like spirometry or body plethysmography require a mouthpiece or facemask, which can be uncomfortable to the test person. As an alternative, we propose to use the change of the geometric shape of the subject's torso while breathing. By acquiring 3D point clouds of the person with a real-time near-infrared (NIR) 3D scanner, we measure those changes in a comfortable, irritation-free, and contact-free manner. Accordingly, two continuously measuring structured light 3D sensors, using a GOBO-based aperiodic sinusoidal pattern projector at a wavelength of 850 nm, simultaneously capture the upper front and side torso of the subject at a frame rate of 200 Hz. Both 3D scanners are calibrated and operated in a sensor network fashion, yielding a unified data stream within a global coordinate system. This results in increased coverage and reduced occlusion of the patient's body shape, enabling robust measurements even in the presence of loose clothing and varying body figure.

We collected data from 16 healthy participants in an upright sitting position, wearing everyday clothing during the measurements. For reference, we simultaneously recorded spirometry readings. An algorithm ("OpTidal") tracks the volume of the subject's torso from the 3D data. Comparison with the reference data shows high correlation and low mean error for the absolute tidal volume readings. As such, our method is a viable, safe, and accurate alternative to spirometry and plethysmography.

Keywords: Tidal volume measurement, optical 3D measurement, contact free, irritation free, spontaneous breathing, OpTidal

1. INTRODUCTION

Optical three-dimensional (3D) measurement systems have become widely adopted in industrial quality control, medical use cases, and cultural heritage applications. The non-contact, dense, and fast 3D point acquisition as well as their high measurement quality qualify pattern projection systems for most of those 3D scanning scenarios. Sensors based on near-infrared (NIR) pattern projection are best suited for irritation-free human monitoring in medical use cases since their illumination is not noticed by the human eye. Recently, continuously and simultaneously measuring systems of multiple 3D scanners, so-called sensor networks, have become feasible. By providing a low-latency, high frame rate data stream of 3D points in a unified coordinate system for large measurement volumes¹, new applications can be explored.

Monitoring the respiratory health or breathing performance of individuals could be an important part in preventive health efforts or a medical survey. Furthermore, they are already important vital signs for patients in intensive care treatment or under high-flow nasal oxygenation⁸. Contactless optical methods offer an advantage over state-of-the-art methods like spirometry or body plethysmography since they don't require a mouthpiece or facemask. This simplifies the measurement of breathing mechanics and is more comfortable to the patient.

1.1 Literature review

As stated by Massaroni², "The most well-established technology to assess the breathing volume of the chest wall and of its compartments (i.e., pulmonary and abdominal rib cage and abdomen) is the optoelectronic plethysmography (OEP)". However, OEP typically still requires the placement of a multitude of (passive reflective) markers onto the

*christoph.munkelt@iof.fraunhofer.de; phone +49 (0)3641 807-245; iof.fraunhofer.de

subject's body, which is time-consuming and requires upper torso exposition. It then tracks these markers to compute the respiratory volume and other breathing-related features.

By optically monitoring the person's body – without markers – directly, even less set-up time is required. Multiple approaches have been examined before. Li et al.^{3,4} have analyzed the performance of an optical surface imaging (OSI) system, comprising three optical sensors typically used in a radiotherapy environment. Such a system measures front and side areas of the upper torso, and merges the overlapping datasets using a rigid registration. They divide the breathing-related volume of interest into chest and belly regions by two cut planes. Furthermore, they use a tilted coronal cut plane to separate the measured patient's body surface from the background. Using this approach and comparing its results to reference spirometric measurements, they could show very good accuracy of this OSI-based motion monitoring technique in this specific radiotherapy laboratory environment. However, access to such measuring capabilities outside this special environment is limited. Furthermore, a more general measurement environment other than lying bare-chested (or wearing a form-fitting leotard), with arms up in a supine position, would be helpful in making the probands more comfortable.

Motamedi-Fakhr et al.⁵ evaluate the application of so-called “structured light plethysmography”, which observes the deformation of a projected grid pattern by two cameras. Such a device, operating in the visible light spectrum and consisting of a single basic scanner, reconstructs the 3D view of chest wall movement during breathing. While the study suggests that breathing patterns from healthy participants can be detected from ones with respiratory diseases, the single sensor approach and the sensitivity to movement artifacts limit its usability. However, a more comfortable measuring scenario (sitting, T-shirt) can be achieved, albeit at a limited coverage and resolution of the underlying reconstructed 3D surface.

In a review by Massaroni et al.⁶ it is stated that “OEP is an accurate and validated method of measuring lung volumes and chest wall movements”. But they also state that marker placement effort and multi-camera OEP system cost needs to be tackled for further extension into applications like exercise sciences and vital parameter monitoring.

The approach proposed by Rehouma et al.⁷ uses two Kinect v2 sensors (time of flight (ToF), using near-infrared (NIR) illumination) to capture the upper torso from two lateral viewpoints. The setup operates in a pediatric intensive care environment and takes its special restrictions into account. The system operates fully contactless and irritation free. To register both sensors, the authors only use one 2D marker. Furthermore, commercial availability of the Kinect v2 and applicability in a medical environment are limited. Using a mannequin with an artificial test lung, the method showed low errors for respiratory rate and tidal volume compared to the reference ventilator values. For real patients requiring mechanical ventilation, the relative errors are much larger, though.

A similar approach, but only using one frontally placed Kinect v2, was recently published by L'Her et al.⁸. They placed a single NIR ToF camera atop patients in intensive care. Some were skin exposed, some were wearing gowns or covered by a blanket. High correlation for both tidal volume and respiratory rate was reported. Furthermore, they use an automatic region-of-interest (RoI) selection to track left / right hemithorax. They propose the system for clinical use cases, e.g., intensive care, specifically patient monitoring under respiratory assistance.

In summary, multiple approaches exist to noninvasively measure or monitor respiratory key characteristics, like tidal volume and respiratory rate. The optoelectronic plethysmography, as the most accurate method, requires too much per-subject effort to be a viable candidate for effectively monitoring breathing characteristics for a multitude of subjects. The ToF-based approaches show potential in a controlled clinical environment. The “structured light plethysmography” approach, operating in the visible spectrum, views the patient only from a single perspective and tracks only a low number of projected features (basically a checkerboard grid).

1.2 Our continuous 3D surface tracking approach

In contrast, our unobtrusive non-contact approach uses two irritation-free NIR-based 3D scanners. Once set up in a 90° angle with the subject at the center, they have a good coverage of the upper torso, including the side and waist area. No per-subject preparations, like marker placement, are necessary, which ensures high throughput in screening scenarios. Subjects don't need to expose the skin; tight or moderately fitting clothing is sufficient. The 3D scanning rate is high enough for respiratory monitoring under light exercise.

Specifically, we use an active illumination 3D reconstruction approach. For each 3D sensor consisting of two 2D cameras, an NIR projector projects a changing pattern using a rotating slide wheel (GOBO (“GOes Before Optics”) principle) with aperiodic sinusoidal fringes (for details, see Heist et al.⁹). Using a sequence of the stripe images, one can easily correlate each pixel between both cameras, thus enabling 3D calculation by triangulation⁹. Furthermore, reconstruction speed is only limited by the available light of the projection engine and the frame rate of the camera system.

Two 3D sensors are combined to have complete coverage of the upper torso. The underlying sensor network¹⁰ unifies the continuously and simultaneously acquired 3D data streams of the two scanners into a global coordinate system. This is achieved by aligning the precisely pre-calibrated 3D sensors using a simple marker-based approach (see Fig. 1) once after sensor installment. This way the sensor system delivers a dense point cloud with 20 Hz 3D frame rate and low latency of ≤ 100 ms (see Munkelt et al.¹). Using this information, changes in the subject's chest wall can be monitored in real time.

2. METHODOLOGY

By monitoring the movement of the subject's chest wall over a timespan t_{total} , we reason on the underlying breathing volume. The state of maximum (V_{max}) and minimum volume (V_{min}) of the chest defines the respective turning points of inhaled or exhaled state. Since the breathing cycle periodically goes through these states, we can determine the number of complete normal breaths n by identifying the extremal values (see the red dots and blue "x" in Fig. 4). The corresponding complete cycle time t_{cyc} reflects the duration of the n breaths within t_{total} . Each complete normal breath has an associated breath volume $V_x = V_{max} - V_{min}$, which reflects the change of chest volume over time. From the average duration of a single full breath period $t_p = n/t_{dur}$, we can calculate the respiratory rate $RR = 60 s/t_p$. From the above, we can calculate the tidal volume TV as follows:

$$TV = \frac{\sum_{x=1}^n V_x \times (60 s/T_{dur})}{RR} \quad (1)$$

To capture a sufficiently large surface area of the front and side torso, two sensors with overlapping fields of view are placed frontally left and right of the subject (see Fig. 3). Thus, even the side areas not present in single-scanner approaches like Motamedi-Fakhr et al.⁵ and L'Her et al.⁸ can be robustly reconstructed. To align the sensors, a series of images of a 2D marker board is captured (see Fig. 1). After subpixel-accurate circle extraction, a Helmert transformation calculates the mapping of the two sensors into a common global coordinate system.

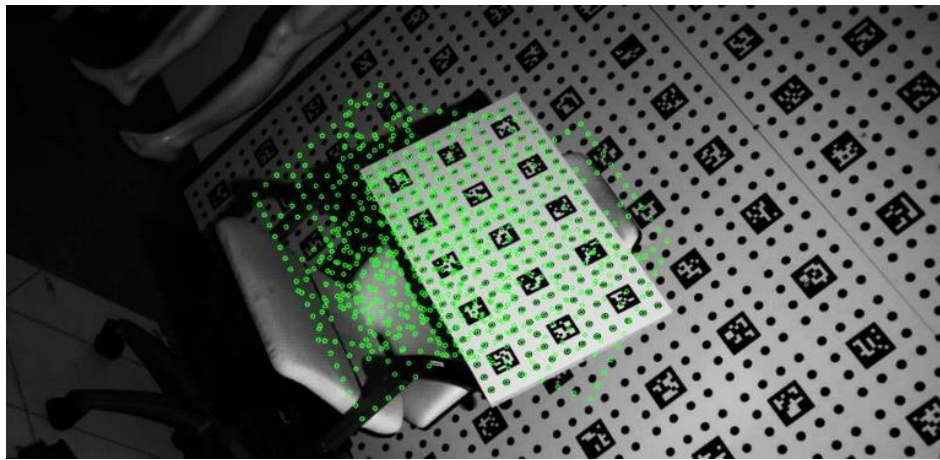


Figure 1. Extrinsic calibration using a small, movable 2D marker board (on chair). 2D image of one camera of the right 3D sensor, where extracted marker positions from multiple board positions are superimposed (green) for illustrative purposes.

Using the unified 3D point cloud of the subject's upper torso, the first step is to place an appropriate region of interest on the relevant area. While this can be done automatically (e.g., using kinematic joint information⁸), we default-positioned a mask, and adjusted size and position if necessary (see Fig. 2 left). The superior boundary was near the clavicle and the inferior boundary was near the pubis. With the sensor network being able to continuously acquire and process dense point clouds from both scanners at 20 Hz, breathing-related motion of the chest wall can be robustly monitored. The reconstructed 3D surface of the RoI is then extracted. For each of its surface elements, the height above the coronal cut plane (gray plane in Fig. 2 right) is back-projected onto the coronal cut plane. The volume is then calculated by the sum of the plane's occupied surface elements' area times their average height above the cut plane. By discretizing the breathing RoI into 100×100 elements, analysis can run in real time with low latency.

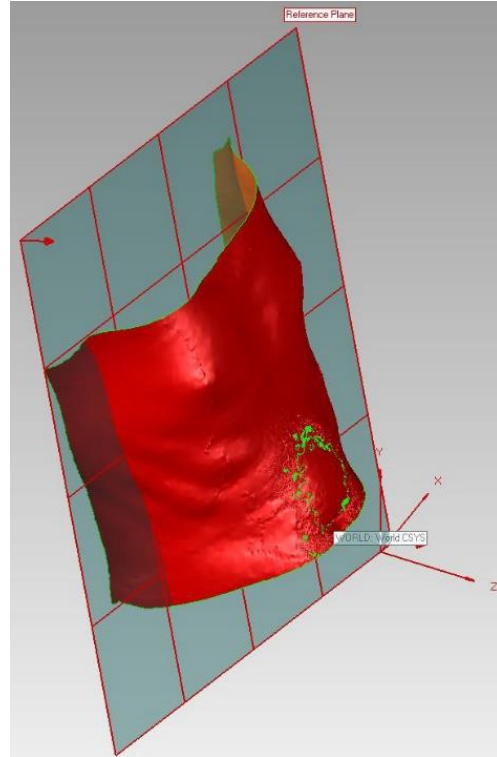
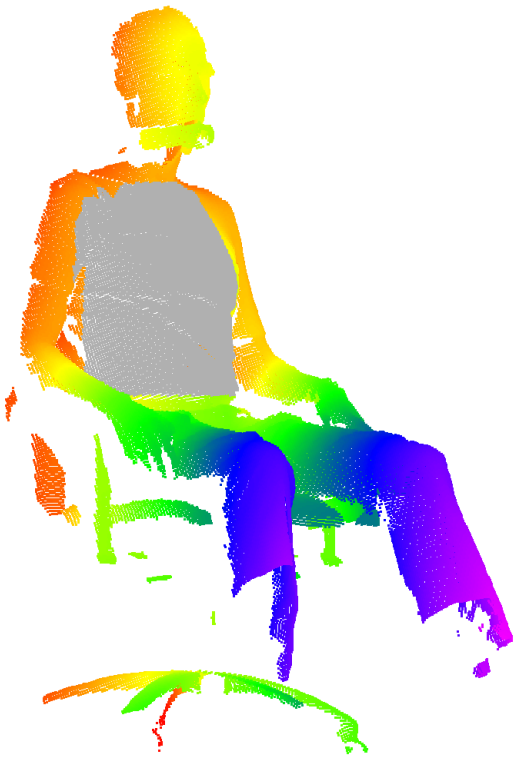


Figure 2. *Left*: Depth-colored 3D reconstruction of sitting person during breath analysis. Mouthpiece present for reference spirometer recordings. Note the grey area: this is the ROI of the upper torso tracked during breath analysis. *Right*: Extracted surface of the ROI on a subject's upper torso. The reference / coronal cut plane is visualized in dark gray in the background.

3. RESULTS

3.1 Experimental setup

To validate our approach, we performed test measurements and analysis on 16 volunteers. The group consisted of 8 healthy women and 8 healthy men. The sensor system was set up in a laboratory as shown in Fig. 3. The two sensors are placed to the left and right in front of a chair. The angle between the sensors is approximately 90° , while the measurement distance is about 3 m. The scanners use GigE-Vision compatible cameras (Baumer VLXT 28M.I) with a native resolution of 1920×1464 pixels. Using the aperiodic sinusoidal stripe illumination at the NIR wavelength of 850 nm at 200 Hz 2D image rate requires operation in 2×2 binning mode, yielding an effective resolution of 960×732 pixels. This setup resulted in a continuous 20 Hz 3D data stream, which was processed online to compute tidal volume TV and respiratory rate RR .

The participants were asked to sit upright (not slouched) and in contact to the back rest of the chair. For reference purposes, they additionally used a spirometer ("Spirolab" from MIR), which directly measures breath flow and volume. Its tube was placed behind the person to not occlude the torso. All participants wore everyday clothing, from T-shirts over shirts to sweaters, not form-fitting leotards. Both measurements, the optical-based ("OpTidal") as well as the spirometer-based ("Spirometer"), were conducted simultaneously. Two of the 16 measurements failed due to spirometer reading failures, the remaining 14 are reported in Table 1.

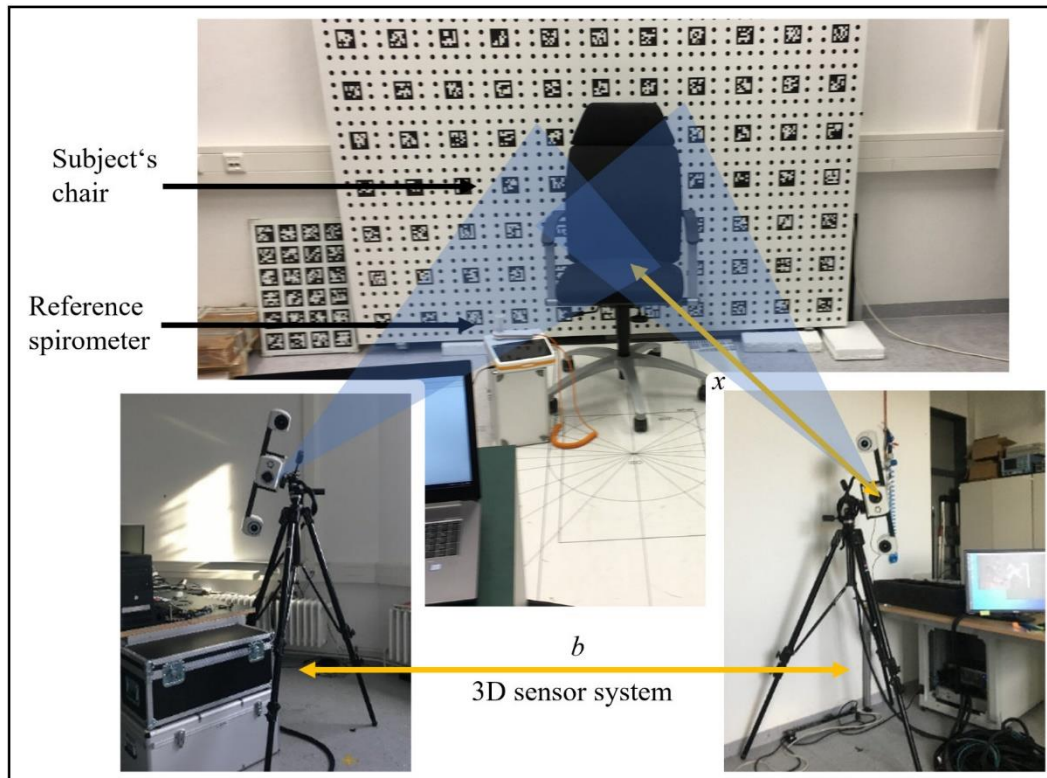


Figure 3. Laboratory scanner setup: two 3D scanners comprising the sensor network. The baseline b (distance between the 3D scanners) is ~ 4 m, the measurement distance x to the proband is ~ 3 m, yielding an inter-sensor angle of approx. 90° .

3.2 Results

The results are shown in Table 1. As can be seen from the cross-correlation coefficient ρ the OpTidal values match the reference Spirometer values very well. Only proband 11, who wore loose-fitting clothing with many creases, shows lower $\rho < 0.9$. Differences in TV between OpTidal and Spirometer methods are lower than 1 l, except for probands 8 and 12. Generally, OpTidal TV tends to underestimate the true tidal volume. This indicates that some breathing effect is not observed in the current setup. Possible reasons are loose-fitting clothing or incomplete masking (e.g., RoI inaccurately set) or incomplete observation (e.g., missing side or back area) of breathing-related body area.

Table 1. Comparison of reference (Spirometer) and OpTidal measurement values.

Proband ID	TV Spirometer (in l)	TV OpTidal (in l)	Correlation coefficient ρ	RR Spirometer (in breaths/min)	RR OpTidal (in breaths/min)
01-male	4.9	4.0	0.99	13.7	13.8
02-male	1.2	0.7	0.96	7.4	8.1
03-male	2.1	1.4	0.96	8.4	8.7
04-female	1.8	1.8	0.91	16.3	14.6
05-female	2.8	2.4	0.95	14.6	14.2
06-female	2.5	3.1	0.99	10.2	10.5
07-female	1.6	1.3	0.97	11.6	11.8
08-male	3.6	2.1	0.97	22.5	22.7
09-female	1.2	1.0	0.99	22.5	22.5

10-male	1.7	1.3	0.98	14.6	14.6
11-female	1.1	0.9	0.83	13.7	15.4
12-male	2.8	1.3	0.99	7.0	7.1
13-female	1.0	0.5	0.98	19.5	19.9
14-male	2.5	1.8	0.97	20.5	21.1

In Fig. 4, two exemplary breathing cycles, synchronously measured by the reference Spirometer (green line) and our OpTidal method (blue fitted line), are displayed. The left subfigure shows the “07-female” dataset, where after an initial discrepancy (first inhale event) between the two methods, we see good accordance both in breathing rate as well as reported volumes. The right subfigure (“10-male” dataset) shows a higher breathing rate and the typical “less volume reported” effect of the OpTidal method. Nevertheless, both measurements illustrate the good correlation between the two methods.

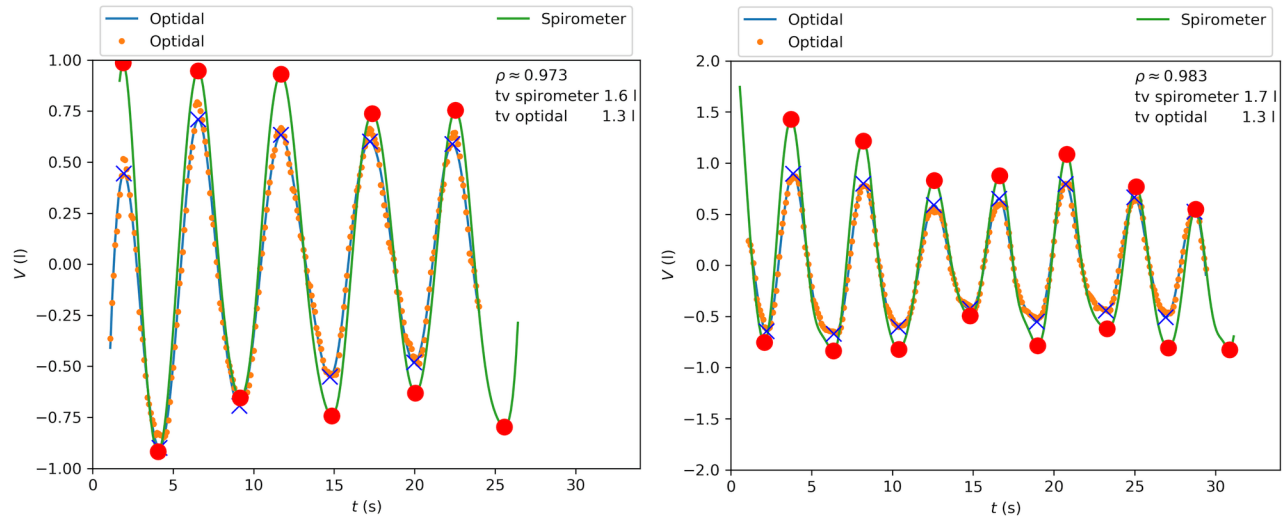


Figure 4. Exemplary test data (left: 07-female, right: 10-male) of our method (OpTidal, orange dots – measurement points, blue – fitted graph, big red dots – extrema) versus reference spirometer (green line – measurements).

3.3 Discussion

Generally, the reported OpTidal measurements are slightly lower than the reference spirometer-based values. Two factors could easily be improved (adaptive RoI instead of a generic one, relatively tight-fitting clothing, e.g., T-shirt). The supposedly not completely scanned body areas, which still contribute to breathing-related volume changes, could be improved by using a chair without armrests as well as by raising the arms above chest level. Additionally, it could be analyzed whether using only one frontally placed 3D scanner yields comparable results. That would decrease coverage but might be compensated by a machine-learning approach. Furthermore, it may enable a favorable compromise between system cost and required accuracy for the intended use case of screening for breathing-related health symptoms.

To improve the system further, we could subdivide the breathing-related body surface (RoI) into left and right hemithoracic region and abdominal region (similar to Li et al.³ and L’Her⁸). That way detection of respiratory and volume distribution abnormalities could be enabled.

4. CONCLUSION

We have shown a method and system (“OpTidal”) to measure the generic biomechanics of breathing in an unobtrusive, fast, contactless, and accurate way. With such a comfortable and effortless procedure, a high number of measurements could be taken in a short time. Since data processing happens on-the-fly, any breathing-related anomalies could be analyzed further on the spot. While we focused on respiratory rate (*RR*) and tidal volume (*TV*), other breathing-related metrics of interest could also be derived. We found a high correlation (typically $\rho > 0.9$) between OpTidal and reference spirometer-based measurements. The employed sensor network, consisting of two irritation-free active-illumination NIR 3D scanners with a 3D frame rate of 20 Hz, robustly and accurately measures breathing-related body surface changes. No special mark-ers or skin exposition were needed. Instead, the subjects wore every-day clothing. Future improvements could target the measurability during light workout, e.g., by enabling higher subject movement robustness by further increasing the 3D measurement rate by 3D sequence length reduction¹¹. Furthermore, the possibility of a more economical and calibration-free single-sensor solution might be investigated.

ACKNOWLEDGMENTS

This work was supported by the Fraunhofer Internal Programs under Grant No. Anti-Corona **066-620000**.

REFERENCES

- [1] Munkelt, C., Heinze, M., Bräuer-Burchardt, C., Kodgirwar, S. P., Kühmstedt, P., and Notni, G., “Large-volume NIR pattern projection sensor for continuous low-latency 3D measurements,” *Dimensional Optical Metrology and Inspection for Practical Applications VIII*, volume 10991K, <https://doi.org/10.1117/12.2518636> (2019).
- [2] Massaroni, C., “The Use of Kinematics for Pulmonary Volume Assessment,” In: Müller B., Wolf S. (eds) *Handbook of Human Motion*. Springer, Cham. https://doi.org/10.1007/978-3-319-14418-4_42 (2018).
- [3] Li, G., Huang, H., Wei, J., Li, D. G., Chen, Q., Gaebler, C. P., Sullivan, J., Zatzky, J., Rimner, A., and Mechalakos, J., “Novel spirometry based on optical surface imaging,” *Med. Phys.* 42 (4), pp. 1690 – 1697. <http://dx.doi.org/10.1118/1.4914391> (2015).
- [4] Li, G., Wei, J., Huang, H., Chen, Q., Gaebler, C. P., Lin, T., Yuan, A., Rimner, A., and Mechalakos, J., “Characterization of optical-surface-imaging-based spirometry for respiratory surrogating in radiotherapy,” *Med. Phys.* 43 (3), pp. 1348 – 1360. <http://dx.doi.org/10.1118/1.4941951> (2016).
- [5] Motamedi-Fakhr, S., Wilson, R. C., Iles, R., “Tidal breathing patterns derived from structured light plethysmography in COPD patients compared with healthy subjects,” *Med Devices (Auckl)*. 2016;10:1-9. <https://doi.org/10.2147/MDER.S119868> (2016).
- [6] Massaroni, C., Carraro, E., Vianello, A., Miccinilli, S., Morrone, M., Levai, I. K., Schena, E., Saccomandi, P., Sterzi, S., Dickinson, J. W., Winter, S., and Silvestri, S., “Optoelectronic Plethysmography in Clinical Practice and Research: A Review,” *Respiration* 2017;93:339-354. <https://doi.org/10.1159/000462916> (2017).
- [7] Rehouma, H., Noumeir, R., Bouachir, W., Jouvét, P., and Essouri, S., “3D imaging system for respiratory monitoring in pediatric intensive care environment,” *Comput Med Imaging Graph.* 2018 Dec;70:17-28. <https://doi.org/10.1016/j.compmedimag.2018.09.006> (2018).
- [8] L’Her, E., Nazir, S., Pateau, V., Visvikis, D., “Accuracy of noncontact surface imaging for tidal volume and respiratory rate measurements in the ICU,” *J Clin Monit Comput.* <https://doi.org/10.1007/s10877-021-00708-x> (2021).
- [9] Heist, S., Dietrich, P., Landmann, M., Kühmstedt, P., Notni, G., Tünnermann, A., “GOBO projection for 3D measurements at highest frame rates: a performance analysis,” *Light Sci Appl* 7, 71; <https://doi.org/10.1038/s41377-018-0072-3> (2018).
- [10] Munkelt, C., Heinze, M., Zimmermann, T., Kühmstedt, P., “High performance, low latency 3D sensor network for live full object reconstruction,” *Proc. SPIE 10667, Dimensional Optical Metrology and Inspection for Practical Applications VII*, 1066706, <https://doi.org/10.1117/12.2305332> (2018).
- [11] Dietrich, P., Munkelt, C., Srokos, K., Landmann, M., Heist, S., Notni, G., “Low latency real time 3D sensor utilizing optimized aperiodic fringe patterns,” *Proc. SPIE 11732, Dimensional Optical Metrology and Inspection for Practical Applications X*, 1173205; <https://doi.org/10.1117/12.2586085> (2021).